AIAA SciTech Forum
11–15 & 19–21 January 2021, VIRTUAL EVENT
AIAA Scitech 2021 Forum

10.2514/6.2021-1701

Spatially and temporally resolved fs/ps CARS measurements of rotation-vibration non-equilibrium in a CH_4/N_2 nanosecond-pulsed discharge

Timothy Y. Chen[1], Benjamin M. Goldberg[2], Christopher J. Kliewer[3], Egemen Kolemen[4], and Yiguang Ju[5]

[1,4-5]*Department of Mechanical and Aerospace Engineering, Princeton University, Princeton, NJ 08544*

[2-3] *Sandia National Laboratories, Livermore, CA 94550*

Abstract: Due to concerns about climate change, there is significant interest to establish CH_4 lean burn engines or convert it to valuable industrial chemicals using non-equilibrium plasmas. To quantitatively understand the dynamics and chemistry of plasma discharge in CH_4 fuel mixtures, it is necessary to obtain time and spatially resolved data of key parameters such as the CH_4 concentration and degree of rotation-vibration non-equilibrium. Rotational fs/ps CARS was used to simultaneously measure rotational and vibrational temperatures of a pin-to-pin 40% CH_4/60% N_2 nanosecond-pulsed discharge at 60 Torr, while the CH_4 concentration was measured by vibrational CARS. The measurement region was 2 mm along the electrode axis, within 150 μm of the cathode surface. Gradients in N_2 rotational and vibrational temperature and CH_4 number density were observed to evolve in time and space. The vibrational temperature peaked above 6000 K, 100 μs after the voltage pulse, and the majority of CH_4 consumption occurred during the voltage pulse. Additional CH_4 consumption along with rapid heating occurred during the first 2 μs of the afterglow, indicating a role of electronically excited N_2 quenching in dissociation of CH_4.

1. Introduction

To prevent global climate temperatures from exceeding 1.5°C, there has been much interest in electrifying industrial chemical processes such as CH_4 reforming and lean burning CH_4 flames for gas turbine engines by using non-equilibrium plasmas [1–6]. However, quantitative understanding of the important reaction pathways in CH_4 reforming has not been achieved due to the lack of model validation metrics measured *in-situ* for even CH_4/N_2 mixtures. Previous work in CH_4/N_2 plasmas were mostly focused on studying chemical processes in Titan's atmosphere [7] and synthesizing materials such as carbon nitride coatings [8]. For model validation, a pulsed discharge is preferable to define a start and end to the discharge as well as to study chemistry in the afterglow. While, pure N_2 or air pulsed discharges have been well-studied and characterized [9–12], only a few studies have explored CH_4/N_2 pulsed plasmas for methane reforming purposes [3,13] or characterized the non-equilibrium state of the plasma [14]. From past numerical

[1] Ph.D. Candidate, tc8@princeton.edu, Student Member AIAA
[2] Postdoctoral Research Associate, presently at Lawrence Livermore National Laboratory
[3] Principal Research Scientist
[4] Assistant Professor
[5] Robert Porter Patterson Professor, Fellow AIAA

simulations, the major dissociation pathway for CH_4 is either through direct electron impact or collisions with electronically excited nitrogen molecules such as $N_2(A)$ [3,13]. However, it is also known that electronic-vibrational (E-V) coupling can be a notable source of vibrational energy in N_2 nanosecond pulsed pin-to-pin discharges [15,16]. Unfortunately, this process was not considered by [3,13], so it is neither clear how quenching of N_2 electronic levels by CH_4 affects the evolution of the rotation-vibration non-equilibrium in N_2, nor is it clear whether there are additional reaction pathways for CH_4 in highly vibrationally excited N_2 mixtures.

Hybrid fs/ps coherent anti-Stokes Raman scattering (fs/ps CARS) is a powerful laser diagnostic capable of probing gas temperature and species concentrations on the picosecond time scale with tens of microns of resolution [17–21]. A methodology for retrieving vibrational and rotational temperatures simultaneously from spatially-resolved 1-D rotational fs/ps CARS images was recently developed [22]. This method takes advantage of the red-shift of rotational energy levels of vibrationally-excited molecules to infer the vibrational temperature along with the rotational temperature. This allows for spatially and time-resolved measurements of rotation-vibration non-equilibrium from one measurement. Additionally, a broadband femtosecond pulse produced from self-phase modulation in a hollow-core fiber was used as the pump/Stokes beam. The generation of Raman coherences up to the C-H stretch of CH_4 was achieved like in past works [19,23]. Therefore, both rotational and vibrational temperatures as well as the CH_4 Q-branch could be measured using the same setup.

In this study, to understand the non-equilibrium dynamics and evolution of the CH_4 number density in a CH_4/N_2 nanosecond-pulsed pin-to-pin discharge, the time-resolved 1-D rotational and vibrational temperatures and CH_4 number densities were measured using fs/ps CARS.

2. Experimental Methods

The detailed experimental setup description and theory behind the detection method is in [22] and only a brief overview will be given here. Hybrid fs/ps CARS takes advantage of the broadband nature of femtosecond laser pulses to probe multiple Raman transitions simultaneously, while the non-resonant background is avoided with a delayed spectrally-narrow probe pulse. In this study, two-beam phase matching is used where the both the pump and Stokes photons come from a single laser source [24]. The principle behind detecting vibrational and rotational temperatures simultaneously from the rotational is given by equations 1-3:

$$\boldsymbol{F(v,J) = B_v\big(J(J+1)\big) - D_v(J^2(J+1)^2)} \quad \textbf{(1)}$$

$$\boldsymbol{B_v = B_e - \alpha\left(v+\frac{1}{2}\right) + \gamma\left(v+\frac{1}{2}\right)} \quad \textbf{(2)}$$

$$\boldsymbol{D_v = D_e + \beta\left(v+\frac{1}{2}\right)} \quad \textbf{(3)}$$

where F is the rotational energy of an N_2 molecule in a state (v,J) with v and J being the vibrational and rotational energy levels, B_v and D_v the vibrational energy level-dependent rotational and centrifugal constants, B_e and D_e are the equilibrium rotational and centrifugal constants, and α, β, and γ are rotation-vibration coupling constants. From equations 1-3, the rotational energy levels exhibit a red-shift with increasing vibrational energy due to the decrease in B_v and increase in D_v. This vibrationally-induced shift can be on the order of 1 cm^{-1}. For molecules in rotation-vibration non-equilibrium, molecules in the excited vibrational states will appear at these shifted wavelengths. Such shifts have been detected before using spontaneous Raman scattering and CARS [25,26]. The shifts can be seen in Fig. 1, where the overall envelope convolution of each of

the peaks with the spectrometer instrument function. Therefore, even without enough resolution to resolve each peak, a one-sided broadening can be detected, which can then be related to the distribution of the vibrational states and its associated vibrational temperature.

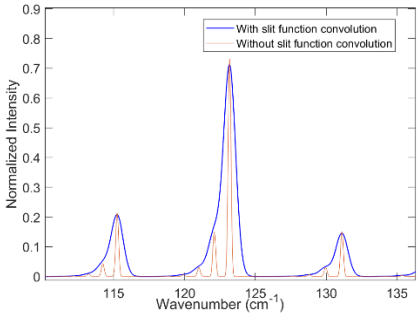

Figure 1. Modelled rotational spectrum at T_r = 400K and T_v = 4000K. The underlying peaks are the fully-resolved shifted vibrationally-excited N_2 lines, while the overarching envelope is the total convolution of the spectrometer instrument with each of the peaks.

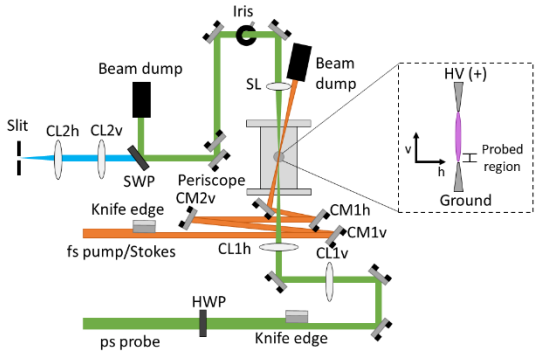

Figure 2. Experimental setup for fs/ps CARS imaging [22]. CM1h, CM1v, CM2v: concave cylindrical mirrors with f= 400 mm, 400 mm, and 200 mm. CL1v, CL1h, CL2v, CL2h: plano-convex cylindrical lenses with f = 300 mm, 400 mm, 400 mm, 75 mm. SL: spherical plano-convex lens with f = 400 mm. SWP: short wave pass.

The fs/ps CARS setup is shown in Fig. 2 and is similar to the setup in [19]. The pump/Stokes photons were generated by focusing 1.5 mJ of a Ti:Sapphire regenerative amplifier into a hollow core fiber (Femtolasers). The output of the fiber was a compressed laser pulse with a pulse width of less than 7 fs and 0.6 mJ of total pulse energy. A picosecond laser with a pulse width of 65 ps and pulse energy of 6 mJ operating at 20 Hz was used as the probe beam. The oscillator of the picosecond laser was phase locked to the oscillator of the femtosecond laser. Knife edges created sharp edges on the incoming beam profiles. The beams were then imaged to the probe volume which reduced light scattering off the cathode surface. The beams were cylindrically focused into sheets and crossed at a 5-degree angle in a 2-beam phase matching configuration. The resulting CARS signal traveled with the probe beam and was separated using an angle-tuned short wave pass filter. The CARS signal was then imaged onto the slit of the spectrometer (Horiba) and detected with a CCD camera (Andor) water-cooled to - 80°C. The plasma was generated by applying a 4 kV, 500 ns pulse from a high voltage switch to the positive electrode (DEI). A 220 Ohm resistor was connected in series between the anode and the high voltage switch to limit the current. The voltage and current traces are shown in Fig. 3 with and without breakdown. The pulses

were applied at 20 Hz and were synchronized with the picosecond laser via a delay generator. CH_4 densities were measured by rotating the grating to the appropriate Raman shift and the signal was integrated across Q-branch region. Measurements at room temperature were taken periodically to serve as a number density calibration.

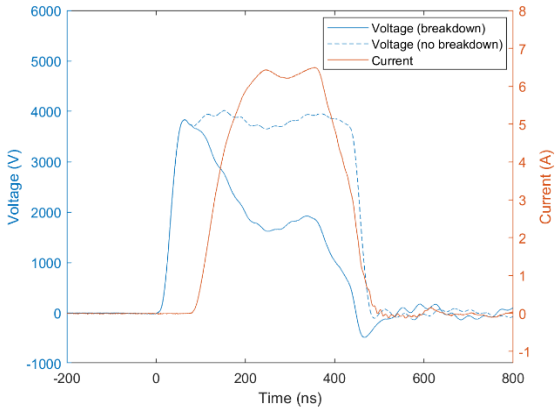

Figure 3. Measured voltage with and without breakdown as well as the conduction current.

3. Results and Discussion

The 1-D time-resolved profiles of the vibrational temperature, rotational temperature, and the CH_4 number density are shown in Fig. 4 and 5. One of the immediately visible trends is that around 100 μs, the vibrational relaxation becomes dominant, with the vibrational temperature decreasing rapidly with the rotational temperature increasing by several hundreds of K. This is more clearly visualized in Fig. 6 by picking a single spatial location, 1500 μm from the cathode, and plotting the time-resolved responses of the three measured parameters. At time scales greater than 100 μs, conduction and diffusion work to smooth the spatial distribution of the rotational temperatures. Additionally, there are strong gradients in the vibrational temperature along the axis of the cathode, reminiscent of a DC glow discharge [27]. This could be possible, since the 500 ns voltage pulse width is much longer than the time to complete the gap, which can occur on tens of ns timescale or faster [28]. Therefore, a transient glow discharge could form, and if the voltage pulse was kept on for longer, transition to an arc would occur [29,30]. For 60 Torr of N_2 and 220 Ohm resistance, the time before the glow-to-arc transition is on the order of a few μs [30]. If we assume that a transient glow has formed, then the region of high vibrational excitation from 600 to 1000 μm corresponds to the negative glow region, where there is a higher electron number density. This would lead to more collisions with neutral molecules and more vibrational excitation through electron-impact. Additionally, this would imply that the cathode sheath thickness is 200-300 μm thick which would be unlikely due to the high conduction current (~ 6 A maximum). Further investigation is required to correlate the discharge structure with the vibrational temperature spatial distribution.

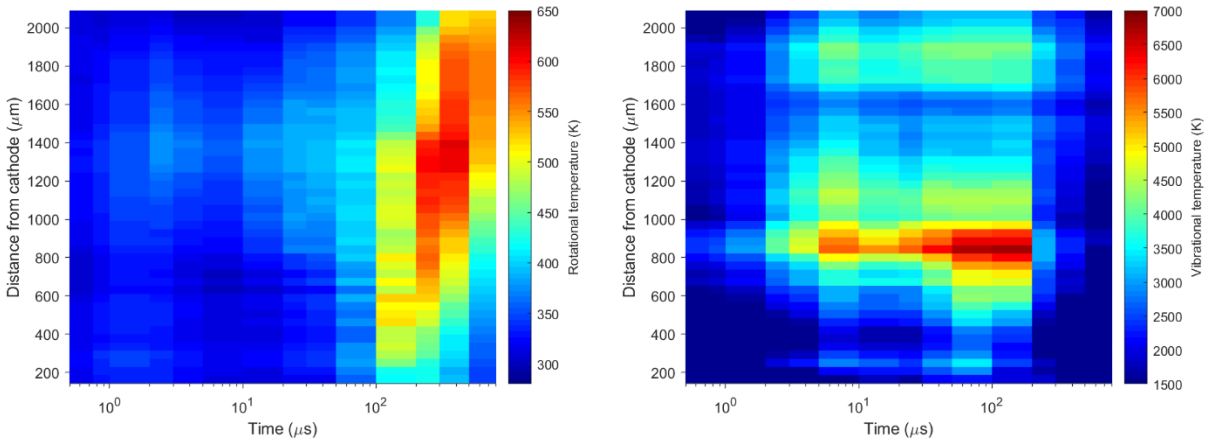

Figure 4. 1-D time-resolved profiles of the rotational (left) and vibrational (right) temperatures. The color bar denotes the temperature at the time marked by the left edge of each cell.

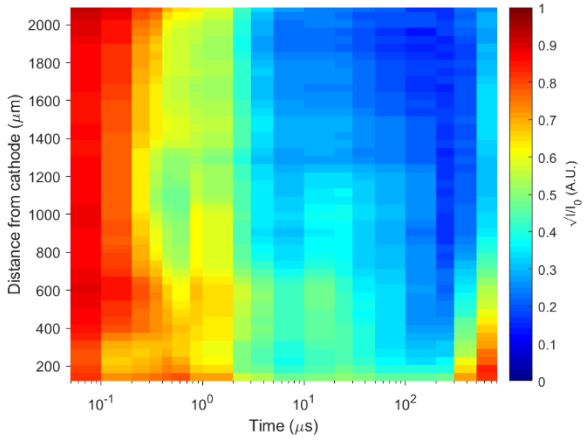

Figure 5. 1-D time-resolved profiles of the square root of the integrated CH_4 signal over the ν_1 Q-branch relative to ambient conditions. The color bar denotes the relative signal at the time marked by the left edge of each cell.

From Figure 6, the CH_4 number density decreased to 50-70% of its starting value within the first 500 ns. This corresponds to the time when the voltage pulse was applied. Afterward, the CH_4 number density fell even more, down to 20-30% of its original value after 10 μs elapsed. At the same time, the rotational temperature did not increase by more than 20%. Therefore, the vast majority of this CH_4 number density decrease was due to dissociation of CH_4 rather than from temperature increase. During the pulse, the dissociation was most likely directly through electron-impact. However, on the μs time scale, the electrons should not have sufficient energy to dissociate CH_4. It is known that electronically excited states of N_2 such as $N_2(A)$ are efficiently produced in high E/N nanosecond-pulsed discharges and collisional quenching leads to "fast gas heating" [31,32]. In air plasmas, fast gas heating occurs due to heat release from N_2 electronic state quenching with O_2, which results in the production of two O atoms. These electronic states also possess sufficient energy to break a C-H bond in CH_4 at a similar rate to using O_2 as the collisional partner [13,31]. Therefore, the rise in temperature and decrease in CH_4 number density after the voltage pulse until 2 μs was most likely due to this quenching. However, this does not explain the further decrease in CH_4 number density, after the end of the fast gas heating. This indicates that

there is an additional reaction pathway consuming approximately 15-20% of the total CH_4 that does not release significant amounts of heat. This decrease occurs during the time when the vibrational temperature increases by more than 1000K. However, between 5 μs and 100 μs, the CH_4 number density remains constant while the vibrational temperature reaches its maximum. Therefore, it is unclear what how the N_2 vibrational kinetics affect the CH_4 number density. Further investigation is required with a chemical kinetic model to fully understand these trends such as in [3].

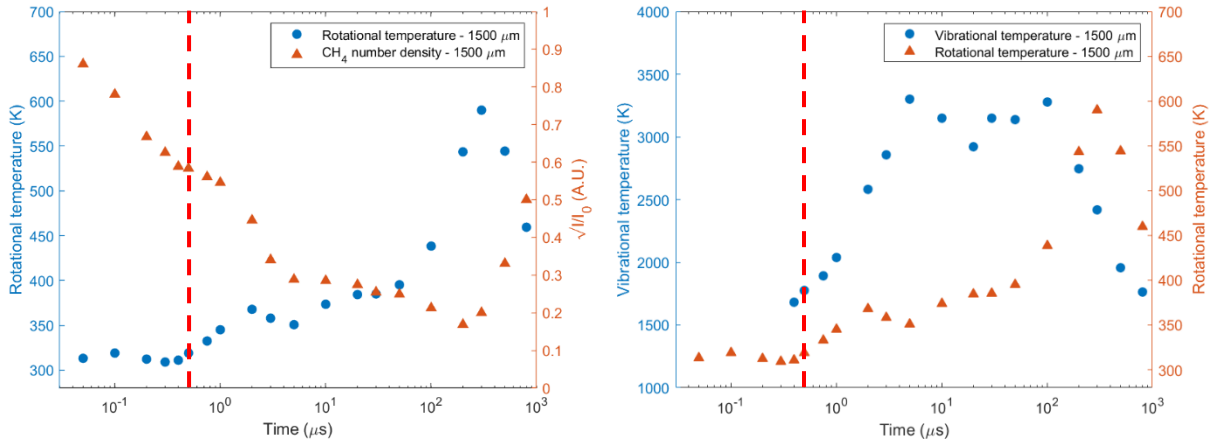

Figure 6. Time-resolved profiles of the CH_4 number density, rotational temperature, and vibrational temperature 1500 μm from the cathode. The red dashed line marks the end of the pulse.

4. Conclusions

In this work, hybrid rotational and vibrational fs/ps CARS was applied to measure the one-dimensional time-evolution of rotational temperature, vibrational temperature, and CH_4 density in a nanosecond-pulsed CH_4/N_2 discharge. From the simultaneous rotational and vibrational temperature measurements, the rotation-vibration relaxation occurred from 100 to 300 μs. From the 1-D vibrational temperatures, strong spatial gradients were observed. Since the applied voltage pulse was much longer than the time to connect the electrode gap, then a transient glow discharge could form after breakdown. Furthermore, from the CH_4 and rotational temperature time evolution, there was evidence for CH_4 dissociation from collisional quenching of electronically excited N_2. However, after the fast gas heating, even more CH_4 consumption occurred, without significant rotational temperature rise. This correlated with an increase in the N_2 vibrational temperature, but during the period of maximum N_2 vibrational temperature, the CH_4 number density was approximately constant. Additional modeling is required to understand how the vibrational kinetics influences the CH_4 conversion.

Acknowledgements

This material is based upon work supported by the U.S. Department of Energy (DOE), Office of Science, Office of Workforce Development for Teachers and Scientists, Office of Science Graduate Student Research (SCGSR) program. The SCGSR program is administered by the Oak Ridge Institute for Science and Education (ORISE) for the DOE. CJK and BMG were supported

by the Office of Chemical Sciences, Geosciences, and Biosciences, Office of Basic Energy Sciences, U.S. Department of Energy. Sandia National Laboratories is a multi-mission laboratory managed and operated by National Technology and Engineering Solutions of Sandia, LLC, a wholly owned subsidiary of Honeywell International, Inc., for the U.S. Department of Energy's National Nuclear Security Administration. YJ would like to thank the funding support of DOE Plasma Science Center, NETL UCFER, and National Science Foundation grants. TYC was partially supported by the Program in Plasma Science and Technology Fellowship (PPST). TYC, EK, and YJ acknowledge the support of ExxonMobil through its membership in the Princeton E-filliates Partnership of the Andlinger Center for Energy and the Environment. We thank Brian D. Patterson for his technical assistance in setting up the fs/ps CARS 1-D imaging apparatus as well as Benjamin T. Yee for lending us the high voltage switch.

References

[1] Scapinello, M., Delikonstantis, E., and Stefanidis, G. D. "The Panorama of Plasma-Assisted Non-Oxidative Methane Reforming." *Chemical Engineering and Processing: Process Intensification*, Vol. 117, 2017, pp. 120–140. https://doi.org/10.1016/j.cep.2017.03.024.

[2] Kameshima, S., Tamura, K., Ishibashi, Y., and Nozaki, T. "Pulsed Dry Methane Reforming in Plasma-Enhanced Catalytic Reaction." *Catalysis Today*, Vol. 256, 2015, pp. 67–75. https://doi.org/10.1016/j.cattod.2015.05.011.

[3] Mao, X., Chen, Q., and Guo, C. "Methane Pyrolysis with N2/Ar/He Diluents in a Repetitively-Pulsed Nanosecond Discharge: Kinetics Development for Plasma Assisted Combustion and Fuel Reforming." *Energy Conversion and Management*, Vol. 200, 2019, p. 112018. https://doi.org/10.1016/j.enconman.2019.112018.

[4] Nozaki, T., and Okazaki, K. "Non-Thermal Plasma Catalysis of Methane: Principles, Energy Efficiency, and Applications." *Catalysis Today*, Vol. 211, 2013, pp. 29–38. https://doi.org/10.1016/j.cattod.2013.04.002.

[5] Ju, Y., and Sun, W. "Plasma Assisted Combustion: Dynamics and Chemistry." *Progress in Energy and Combustion Science*, Vol. 48, 2015, pp. 21–83. https://doi.org/10.1016/j.pecs.2014.12.002.

[6] Kim, W., Godfrey Mungal, M., and Cappelli, M. A. "The Role of in Situ Reforming in Plasma Enhanced Ultra Lean Premixed Methane/Air Flames." *Combustion and Flame*, Vol. 157, No. 2, 2010, pp. 374–383. https://doi.org/10.1016/j.combustflame.2009.06.016.

[7] Pintassilgo, C. D., and Loureiro, J. "Kinetic Study of a N2–CH4 Afterglow Plasma for Production of N-Containing Hydrocarbon Species of Titan's Atmosphere." *Advances in Space Research*, Vol. 46, No. 5, 2010, pp. 657–671. https://doi.org/10.1016/j.asr.2010.04.027.

[8] Pereira, J., Géraud-Grenier, I., Massereau-Guilbaud, V., Plain, A., and Fernandez, V. "Characterization of A-CNx:H Particles and Coatings Prepared in a CH4/N2 r.f. Plasma." *Surface and Coatings Technology*, Vol. 200, Nos. 22–23, 2006, pp. 6414–6419. https://doi.org/10.1016/j.surfcoat.2005.11.004.

[9] Pai, D. Z., Stancu, G. D., Lacoste, D. A., and Laux, C. O. "Nanosecond Repetitively Pulsed Discharges in Air at Atmospheric Pressure—the Glow Regime." *Plasma Sources Science and Technology*, Vol. 18, No. 4, 2009, p. 045030. https://doi.org/10.1088/0963-0252/18/4/045030.

[10] Pai, D. Z., Lacoste, D. A., and Laux, C. O. "Nanosecond Repetitively Pulsed Discharges in Air at Atmospheric Pressure—the Spark Regime." *Plasma Sources Science and Technology*, Vol. 19, No. 6, 2010, p. 065015. https://doi.org/10.1088/0963-0252/19/6/065015.

[11] Lempert, W. R., and Adamovich, I. V. "Coherent Anti-Stokes Raman Scattering and Spontaneous Raman Scattering Diagnostics of Nonequilibrium Plasmas and Flows." *Journal of Physics D: Applied Physics*, Vol. 47, No. 43, 2014, p. 433001. https://doi.org/10.1088/0022-3727/47/43/433001.

[12] Teramoto, Y., and Ono, R. "Measurement of Vibrationally Excited N_2 (v) in an Atmospheric-Pressure Air Pulsed Corona Discharge Using Coherent Anti-Stokes Raman Scattering." *Journal of Applied Physics*, Vol. 116, No. 7, 2014, p. 073302. https://doi.org/10.1063/1.4893474.

[13] Snoeckx, R., Setareh, M., Aerts, R., Simon, P., Maghari, A., and Bogaerts, A. "Influence of N2 Concentration in a CH4/N2 Dielectric Barrier Discharge Used for CH4 Conversion into H2." *International Journal of Hydrogen Energy*, Vol. 38, No. 36, 2013, pp. 16098–16120. https://doi.org/10.1016/j.ijhydene.2013.09.136.

[14] Chen, T. Y., Rousso, A. C., Wu, S., Goldberg, B. M., van der Meiden, H., Ju, Y., and Kolemen, E. "Time-Resolved Characterization of Plasma Properties in a CH_4 /He Nanosecond-Pulsed Dielectric Barrier Discharge." *Journal of Physics D: Applied Physics*, Vol. 52, No. 18, 2019, p. 18LT02. https://doi.org/10.1088/1361-6463/ab0598.

[15] Montello, A., Yin, Z., Burnette, D., Adamovich, I. V., and Lempert, W. R. "Picosecond CARS Measurements of Nitrogen Vibrational Loading and Rotational/Translational Temperature in Non-Equilibrium Discharges." *Journal of Physics D: Applied Physics*, Vol. 46, No. 46, 2013, p. 464002. https://doi.org/10.1088/0022-3727/46/46/464002.

[16] Wu, Y., Limbach, C., Tropina, A., and Miles, R. Space and Time Analysis of the N_2 Vibrational Non-Equilibrium in the N_2 and Air Nanosecond Discharge Afterglow. Presented at the AIAA Scitech 2019 Forum, San Diego, California, 2019.

[17] Prince, B. D., Chakraborty, A., Prince, B. M., and Stauffer, H. U. "Development of Simultaneous Frequency- and Time-Resolved Coherent Anti-Stokes Raman Scattering for Ultrafast Detection of Molecular Raman Spectra." *The Journal of Chemical Physics*, Vol. 125, No. 4, 2006, p. 044502. https://doi.org/10.1063/1.2219439.

[18] Stauffer, H. U., Miller, J. D., Slipchenko, M. N., Meyer, T. R., Prince, B. D., Roy, S., and Gord, J. R. "Time- and Frequency-Dependent Model of Time-Resolved Coherent Anti-Stokes Raman Scattering (CARS) with a Picosecond-Duration Probe Pulse." *The Journal of Chemical Physics*, Vol. 140, No. 2, 2014, p. 024316. https://doi.org/10.1063/1.4860475.

[19] Bohlin, A., and Kliewer, C. J. "Direct Coherent Raman Temperature Imaging and Wideband Chemical Detection in a Hydrocarbon Flat Flame." *The Journal of Physical Chemistry Letters*, Vol. 6, No. 4, 2015, pp. 643–649. https://doi.org/10.1021/acs.jpclett.5b00014.

[20] Dedic, C. E., Meyer, T. R., and Michael, J. B. "Single-Shot Ultrafast Coherent Anti-Stokes Raman Scattering of Vibrational/Rotational Nonequilibrium." *Optica*, Vol. 4, No. 5, 2017, p. 563. https://doi.org/10.1364/OPTICA.4.000563.

[21] Retter, J. E., Elliott, G. S., and Kearney, S. P. "Dielectric-Barrier-Discharge Plasma-Assisted Hydrogen Diffusion Flame. Part 1: Temperature, Oxygen, and Fuel Measurements by One-Dimensional Fs/Ps Rotational CARS Imaging." *Combustion and Flame*, Vol. 191, 2018, pp. 527–540. https://doi.org/10.1016/j.combustflame.2018.01.031.

[22] Chen, T. Y., Goldberg, B. M., Patterson, B. D., Kolemen, E., Ju, Y., and Kliewer, C. J. "1-D Imaging of Rotation-Vibration Non-Equilibrium from Pure Rotational Ultrafast Coherent Anti-Stokes Raman Scattering." *Optics Letters*, 45, 4252-4255, 2020.
[23] Bohlin, A., Jainski, C., Patterson, B. D., Dreizler, A., and Kliewer, C. J. "Multiparameter Spatio-Thermochemical Probing of Flame–Wall Interactions Advanced with Coherent Raman Imaging." *Proceedings of the Combustion Institute*, Vol. 36, No. 3, 2017, pp. 4557–4564. https://doi.org/10.1016/j.proci.2016.07.062.
[24] Bohlin, A., and Kliewer, C. J. "Two-Beam Ultrabroadband Coherent Anti-Stokes Raman Spectroscopy for High Resolution Gas-Phase Multiplex Imaging." *Applied Physics Letters*, Vol. 104, No. 3, 2014, p. 031107. https://doi.org/10.1063/1.4862980.
[25] Barrett, J. J., and Harvey, A. B. "Vibrational and Rotational–Translational Temperatures in N2 by Interferometric Measurement of the Pure Rotational Raman Effect." *Journal of the Optical Society of America*, Vol. 65, No. 4, 1975, p. 392. https://doi.org/10.1364/JOSA.65.000392.
[26] Teets, R. E., and Bechtel, J. H. "Coherent Anti-Stokes Raman Spectra of Oxygen Atoms in Flames." *Optics Letters*, Vol. 6, No. 10, 1981, p. 458. https://doi.org/10.1364/OL.6.000458.
[27] Raizer, Y. P., and Allen, J. E. *Gas Discharge Physics*. Springer Berlin, 1997.
[28] Tholin, F., and Bourdon, A. "Influence of Temperature on the Glow Regime of a Discharge in Air at Atmospheric Pressure between Two Point Electrodes." *Journal of Physics D: Applied Physics*, Vol. 44, No. 38, 2011, p. 385203. https://doi.org/10.1088/0022-3727/44/38/385203.
[29] Chalmers, I. D. "The Transient Glow Discharge in Nitrogen and Dry Air." *Journal of Physics D: Applied Physics*, Vol. 4, No. 8, 1971, pp. 1147–1151. https://doi.org/10.1088/0022-3727/4/8/314.
[30] Fujiwara, T., Sato, T., Sekikawa, J., and Yamada, H. "Transient Glow Discharge in Nitrogen after the Breakdown." *Journal of Physics D: Applied Physics*, Vol. 27, No. 4, 1994, pp. 826–829. https://doi.org/10.1088/0022-3727/27/4/021.
[31] Popov, N. A. "Investigation of the Mechanism for Rapid Heating of Nitrogen and Air in Gas Discharges." *Plasma Physics Reports*, Vol. 27, No. 10, 2001, pp. 886–896. https://doi.org/10.1134/1.1409722.
[32] Lanier, S., Shkurenkov, I., Adamovich, I. V., and Lempert, W. R. "Two-Stage Energy Thermalization Mechanism in Nanosecond Pulse Discharges in Air and Hydrogen–Air Mixtures." *Plasma Sources Science and Technology*, Vol. 24, No. 2, 2015, p. 025005. https://doi.org/10.1088/0963-0252/24/2/025005.